Global Investigation of p53-induced Apoptosis Through Quantitative Proteomic Profiling Using Comparative Amino Acid-coded Tagging*[S]

Sheng Gu‡§, Zhihe Liu¶§, Songqin Pan‡, Zeyu Jiang‖, Huimei Lu¶, Or Amit¶, E. Morton Bradbury‡, Chien-An A. Hu¶‡‡, and Xian Chen‡ ‡‡**

p53-induced apoptosis plays a pivotal role in the suppression of tumorigenesis, and mutations in p53 have been found in more than 50% of human tumors. By comparing the proteome of a human colorectal cancer cell transfected with inducible p53 (DLD-1.p53) with that of the control DLD-1 cell line using amino acid-coded mass tagging (AACT)-assisted mass spectrometry, we have broadly identified proteins that are upregulated at the execution stage of the p53-mediated apoptosis. In cell culturing, the deuterium-labeled (heavy) amino acids were incorporated into the proteome of the induced DLD-1.p53 cells, whereas the DLD-1.vector cells were grown in the unlabeled medium. In high-throughput LC-ESI-MS/MS analyses, the AACT-containing peptides were paired with their unlabeled counterparts, and their relative spectral intensities, reflecting the differential protein expression, were quantified. In addition, our novel AACT-MS method utilized a number of different heavy amino acids as internal markers that significantly increased the peptide sequence coverage for both quantitation and identification purposes. As a result, we were able to identify differentially regulated protein isozymes that would be difficult to distinguish by ICAT-MS methods and to obtain a large dataset of the proteins with altered expression in the late stage of p53-induced apoptosis. The regulated proteins we identified are associated with several distinct functional categories: cell cycle arrest and p53 binding, protein chaperoning, plasma membrane dynamics, stress response, antioxidant enzymes, and anaerobic glycolysis. This result suggests that the p53-induced apoptosis involves the *systematic* activation of *multiple* pathways that are glycolysis-relevant, energy-dependent, oxidative stress-mediated, and possibly mediated through interorganelle crosstalks. *Molecular & Cellular Proteomics 3: 998–1008, 2004.*

From the ‡MS M888, B-2, Bioscience Division, Los Alamos National Laboratory, Los Alamos, NM 87545; ¶Department of Biochemistry and Molecular Biology, University of New Mexico Health Sciences Center, Albuquerque, NM 87131; ‖Bioinformatics Division, Department of Biochemistry and Molecular Biology, University of New Mexico Health Sciences Center, Albuquerque, NM 87131; and **Department of Biochemistry and Molecular Medicine, School of Medicine, University of California at Davis, Davis, CA 95616

Received, February 27, 2004, and in revised form, July 19, 2004
Published, MCP Papers in Press, July 28, 2004, DOI 10.1074/mcp.M400033-MCP200

Apoptosis or programmed cell death is an essential and highly regulated physiological process that is required for the normal development and maintenance of tissue homeostasis in all multicellular organisms. The function of this process is to eliminate unwanted or injured cells with characteristic cellular and biochemical hallmarks. Dysregulation of apoptosis is evident in many human diseases including cancer, neurodegenerative disorders, and acquired immune deficiency syndrome (1–4).

In mammals, there are at least three distinct but interactive and interconnected apoptotic pathways: mitochondrial-mediated, death receptor-initiated, and endoplasmic reticulum stress-mediated pathways (2, 5). In the mitochondrial pathway, death signals induce: 1) a variety of protein responses (*e.g.* posttranslational modifications, conformational changes, interorganelle translocations of specific proteins); 2) changes in mitochondrial membrane permeability (MMP)[1]; and 3) the release of apoptogenic factors (*e.g.* cytochrome *c*, apoptosis inducing factor) that activate caspases (1, 2, 5, 6). All cell types, except for mature red blood cells, exhibit mitochondrial-mediated apoptosis. p53, a tumor suppressor protein and a transactivating factor, plays a pivotal role in regulating cell cycle arrest, differentiation, and apoptosis. Mutations in p53 have been found in more than 50% of human tumors (7, 8). The elevated expression of p53 leads to mitochondrial-mediated apoptosis, in part, through the generation of reactive oxygen species (ROS) and oxidative stress. Genes that are directly involved in the generation of ROS are induced in p53-mediated apoptotic pathways (3, 9). For example, the overexpression of one of the p53-inducible genes, proline oxidase, in the inducible colorectal cancer cell line (DLD-1), triggers ROS generation and apoptosis (10, 11).

Previously, systematic investigation of p53-induced apoptosis has been explored by four different genomic methodologies: serial analysis of gene expression (9, 12), microarray

[1] The abbreviations used are: MMP, mitochondrial membrane permeability; ROS, reactive oxygen species; AACT, amino acid coded mass tagging; NCBI, National Center for Biotechnology Information; Hsp, heat shock protein; ANT, adenosine nucleotide translocator; Cyp, cyclophilin; VDAC, voltage-directed anion channel; HBSS, Hanks' balanced salt solution; GAPDH, glyceraldehydes-3-phosphate dehydrogenase; PK, pyruvate kinase; GK, glucokinase; PT, permeability pore.

(13), differential display (14), and subtractive hybridization (15). Approximately 150 genes have been shown to be transcriptionally upregulated by p53. They generally fall into three groups based on their subcellular locations (7): annexin V, CD95, and KILLER/DR5 in the cell membrane; p53-inducible genes in the cytoplasm; and NOXA and PUMA in the mitochondria. However, few of these genes have been characterized directly at the protein level. In general, although a systematic analysis of mRNA expression can provide a profile of a cell/tissue transcriptome, there may be poor correlations between mRNAs and protein abundances (16). Moreover, quantitative mRNA levels are insufficient to predict actual protein expressions because of post-transcriptional regulation and internal ribosome initiation of translation (17, 18). Finally, proteins are subjected to post-translational modifications, and their stabilities are regulated over a range of physiological conditions.

MS-based approaches have emerged as powerful tools for the genome-wide profiling of cellular or organism proteins (19). Two-dimensional electrophoresis comparisons of the protein expression patterns between the normal and diseased tissues or before and after therapeutic treatment allow for the identification of proteins involved in pathogenesis (20). Without using a two-dimensional gel electrophoresis display, direct protein quantitation based on MS signals remains a challenging problem because of the nonlinear correlation between protein quantity and MS signal intensity. Therefore, a number of isotope-tagging methods, such as ICAT, have been introduced to provide MS-recognizable markers/references in protein quantification (21, 22). The strategy of amino acid-coded mass tagging (AACT) (23) or stable isotope labeling by amino acids in cell culture (24) with stable isotopes through *in vivo* cell culturing provides a more accurate and comprehensive approach for quantitative proteome analyses (25–27). We coupled this AACT strategy with both LC-MS/MS and MALDI-TOF MS to profile global protein expression changes in p53-induced apoptosis in a human colorectal cancer cell line that harbors an inducible p53 gene.

EXPERIMENTAL PROCEDURES

Chemicals and Reagents—The deuterium-labeled amino acids, [5,5,5-d_3]leucine (leu-d_3), [4,4,5,5-d_4]lysine (lys-d_4), [methyl-d_3]methionine (met-d_3), and [3,3-d_2]tyrosine (tyr-d_2) were purchased from Cambridge Isotope (Andover, MA). Trypsin was purchased from Roche Diagnostics Corporation (Basel, Switzerland). All components, except hygromycin B (Calbiochem, Darmstadt, Germany) and doxycycline (Sigma, St. Louis, MO) of the cell culture medium such as α-MEM medium, regular and dialyzed fetal bovine serum (FBS), geneticin (G418), penicillin, and streptomycin were obtained from Invitrogen (Carlsbad, CA). C_{18} ZipTips were purchased from Millipore (Billerica, MA). Other chemicals for SDS-PAGE gel electrophoresis, peptide extraction, and sample preparation for MALDI-TOF and ESI-LC-MS were purchased from Sigma. The antibodies used in immunoblotting and immunofluorescence studies were purchased from Santa Cruz Biotechnology (Santa Cruz, CA), Calbiochem, and Bioreagents as indicated. All the chemicals were sequence- or HPLC-grade unless specifically mentioned.

Cell Culturing, In Vivo AACT, and Apoptosis Induction—Stably transfected DLD-1.p53 and DLD-1.vector cells are "Tet-Off" inducible systems as described (10, 28). The normal DLD-1. vector cells were first maintained in the α-MEM medium supplemented with 10% dialyzed fetal bovine serum, 100 units/ml penicillin, and 100 μg/ml streptomycin sulfate in the presence of 20 ng/ml doxycycline, at 37 °C with 5% CO_2 and 90% humidity. The inducible DLD-1.p53 cells were cultured in the AACT-α-MEM, *i.e.*, the selected deuterium-labeled amino acid was added to substitute its unlabeled counterpart depleted in the α-MEM (25). At about 60% confluence, the adherent cells were rinsed in PBS and re-fed with the induction medium, *i.e.,* AACT-α-MEM in the absence of doxycycline, for the induction of p53 and apoptosis for 22 h.

Protein Separation—Equal numbers of the induced AACT-labeled DLD-1.p53 and the unlabeled DLD-1.vector cells were mixed and lysed in 1× SDS-PAGE loading buffer. Two hundred micrograms of total protein were separated on 12% one-dimensional SDS-PAGE and stained with Coomassie blue R-250. Protein bands were excised continuously with a 1–2 mm step from 10 kDa to the loading well.

MALDI-TOF and μLC-Nanospray-MS Analysis—A total of 39 bands were excised. Trypsin digestion and peptide extraction were carried out as previously described (29, 30). The pellets were resuspended in 20 μl of 0.1% TFA solution for MS analysis. For MALDI-TOF MS analysis, additional desalting steps were performed using C_{18} ZipTips and mass spectra were acquired as previously described (29, 30) with a PE Voyager DE_STR biospectrometry work station. HPLC-MS were carried out as previously described (31) on a μLC-nanospray-MS/MS using a QSTAR Pulsar I mass spectrometer (Applied Biosystems, Foster City, CA) coupled with LC Packings Ultimate μLC system (Dionex, Sunnyvale, CA). Five microliters of sample was loaded on the column for analysis.

Protein Identification and Quantitative Analysis—Both MASCOT (ver 1.9.2) (Matrix Science, Boston, MA) and ProID (ver 1.1) (Applied Biosystems) programs were used to interpret the LC-MS/MS data by searching against the National Center for Biotechnology Information (NCBI) human protein database. The AACT modifications were added in the configuration file to allow them to be chosen for the database searching. The parameters for database searching were as follows: 1) 100 ppm mass error tolerance for both MS and MS/MS; 2) variable modifications including phosphorylations of tyrosine/serine/threonine, oxidation of methionine, and the AACT modified precursors; 3) one miscleavage of tryptic enzyme specificity was allowed; 4) peaks with intensities less than 0.5% of the base peak in MS/MS were ignored for database searches; and 5) no smoothing of spectra was applied. Peptide matches with significant homology ($p < 0.05$) (32) were considered as identified peptides. Proteins with two or more matched peptides were classified as validated identification. Only top rank peptide hits for given precursors were used for further protein identifications. The proteins identified by single-peptide MS/MS were validated by manual inspection of the spectra.

The spectra of those peptides containing the labeled precursors were further analyzed for protein quantification. The raw MS/MS data were manually inspected for the best match between the peptide sequence revealed in the first-round search and the corresponding mass-split pattern. This process validates the database search result, and meanwhile the quantitative measurements can be obtained by two approaches. One is to average all the TOF MS spectra of both the light and heavy forms of the peptides with the quantitative results obtained by comparing their mono-isotopic peak intensities. The other approach is to examine chromatographic (extract ion current) profiles of both forms of the peptides. Quantitative results can be obtained by comparing the integral peak areas of unlabeled and labeled peptides. In our study, these two approaches gave similar results. However, mass spectra that showed severe signal overlap-

ping in mass spectra were not included in the results.

For those low-abundance proteins whose peptide signals were only observed by MALDI-TOF MS, AACT-constrained peptide mass fingerprint searches were used to identify proteins from the MALDI-TOF-generated dataset (30). For all the peptides that displayed more intense heavy isotope peaks relative to their light form in MALDI-TOF MS, the observed *m/z* and peptide composition were submitted to the NCBI nonredundant database to determine the protein identity with the modest mass tolerance (300 ppm for external calibrated spectra, 100 ppm for internal calibrated spectra) using the MS-Seq program (30).

Immunoblotting and Immunofluorescent Microscopy Analysis—Total soluble protein extracts were separated using 10 or 12% SDS-PAGE (250 μg protein/lane) and transferred to nylon membranes (Millipore), which were then incubated with commercially available antisera against primary antibodies purchased directly from the suppliers: heat shock protein (Hsp) 10 (rabbit polyclonal, C-20), Hsp27 & Hsp70 (mouse monoclonal), and adenosine nucleotide translocator (ANT) (rabbit polyclonal) from Santa Cruz Biotechnology; cyclophilin (Cyp)A (rabbit polyclonal), CypD (rabbit polyclonal) and voltage-directed anion channel (VDAC) (anti-porin 31 HL, mouse monoclonal) from Calbiochem; and CypB (rabbit polyclonal) from Bioreagents. In the standard assay, we used rabbit polyclonal antisera (1:500) or mouse monoclonal antisera (1:500) for the primary antibody and goat anti-rabbit horseradish peroxidase or anti-mouse horseradish peroxidase as the secondary antibody (1:5,000) (BioRad). For the immunofluorescence study, DLD-1.p53 cells were cultured on glass coverslips coated with collagen (Roche Diagnostics). After induction for 22 h, the cells were rinsed with Hanks' balanced salt solution (HBSS) and then fixed with 4% paraformaldehyde (w/v) solution at room temperature. Coverslips were rinsed twice with HBSS and blocked with 3% (w/v) BSA for 30 min at room temperature. After incubation with the primary antibody in 3% BSA overnight at 4 °C, coverslips were rinsed with HBSS four times and incubated with Texas Red-labeled anti-IgG secondary antibody (1:200; Vector Laboratories, Burlingame, CA) in 3% BSA for 1 h at room temperature. Coverslips were rinsed with HBSS, mounted onto the slide, and subjected to fluorescent microscope analysis.

RESULTS AND DISCUSSION

Large-scale Analyses of Differentially Expressed Proteins in Response to p53 Overexpression Using AACT-assisted μLC-MS/MS—As previously described (25), the control DLD-1 cells were grown in the α-MEM medium containing natural amino acids (light), whereas the DLD-1.p53 cells were cultured in the same medium except for the substitution of a particular type of amino acid with its deuterated analogue (heavy). The "light" isotope peaks are derived from proteins expressed in the light medium, whereas their "heavy" counterparts corresponded to proteins derived from the p53-induced, apoptotic DLD-1.p53 cells. The rationale for studying the 22-h time point is because p53 is multifunctional. Overexpression of p53 induces cell cycle arrest, apoptosis, and differentiation simultaneously. We intended to identify those proteins that are regulated at the execution (late) stage of apoptosis. Overexpression of p53 for 22 h induced cell death in about 50% of the cells (data not shown) (28).

In-gel tryptic digestions were performed on 39 bands excised from the one-dimensional SDS gel of the lysate extracted from a mixture of equal numbers of labeled and unlabeled cells. Peptides eluted from each gel slice were analyzed by nano-spray μLC-MS/MS. More than 20,000 MS/MS spectra were collected from these LC-MS/MS runs. The mass-tagged proteins expressed in DLD-1.p53 cells were found to be highly specific, and ~50% of the total peptides detected by MS contained either leu-d_3 or lys-d_4 tags.

Note that for those proteins matched with a single peptide MS/MS spectrum, manual inspections were used with the following criteria: 1) individual peptide score should be higher than the identification threshold set in the database searching ($p < 0.05$); 2) both N- and C-terminal fragment ions should be presented in each raw spectrum; and 3) at least 4–5 continuous b- or y- ions should be observed in each raw spectrum. As a result, 417 proteins were identified as nonredundant proteins (Supplemental Table I). These identifications were further validated by searching against a reversed sequence NCBI human protein database according Gygi's method to evaluate a large set of LC-MS/MS data (33). No hit passes the stringent criteria described above.

Quantitative Criteria for Determining Regulated Proteins—Differential protein expressions induced by p53 overexpression were quantitated by comparing the intensity of an AACT peptide with that of its unlabeled counterpart. During μLC separations, most of the AACT peptides co-eluted from the LC column with their unlabeled counterparts; the labeled peptides usually eluted slightly ahead by 1–5 s. We averaged the chromatographic profiles of both isotope peptides rather than using single time spectra for quantitative analyses. For those peptides containing only a single leucine residue, the M^+ ion peak of the labeled peptide could overlap with the $(M+3)^+$ peak of the unlabeled peptide. Therefore, to ensure accuracy of quantitation, the theoretical intensity of the $(M+3)^+$ peak of each unlabeled peptide was calculated from its atomic compositions and then subtracted from the observed peak intensity to give the real intensity of the labeled peak.

Both leucine and lysine are widely distributed residues in cellular proteins. Leucine residue constitutes 9.1% in human proteome, and the average length of a tryptic peptide is ~11 amino acids (34); therefore, each tryptic peptide might contain one leucine. In most cases, mass tagging with heavy leucine resulted in multiple labeled peptide signals, which enhanced the accuracy for protein quantification and identification. Among the identified 417 proteins, more than half of them were quantified by using AACT. Because almost all tryptic peptides have either lysine or arginine at their C termini, using lysine and arginine tags as a pair will provide close to 100% quantifying coverage for all identified proteins.

We used various bioassays to validate the AACT-based quantitative results close to the lower limit, which is defined by at least 20% differential protein expression (see Table I and Fig. 3). The linear range of comparative protein quantitation using the AACT method is 25-fold as demonstrated previously (26). For good signal-to-noise ratios, accurate quantitative measurements were obtained within the linear response

TABLE I
Up-regulated proteins in p53-induced apoptosis

Category	Protein description	NCBI nonredundant accession number	H:L ratio[a]	S.D.[b]	Number of matched peptides	Number of precursor-containing peptides	Method[c]
Cell-cycle arrest and p53 binding	14-3-3 σ	gi 398953	2.21	0.19	5	4	A
Protein chaperoning and configuration	Heat shock protein 70 (HSP70)	gi 462325	1.43	0.12	13	10	A
	Heat shock protein 27 (HSP27)	gi 19855073	2.68	0.27	4	3	A
	Heat shock cognate protein 54 (HSC54)	gi 11526573	1.43	0.06	9	7	A
	Cyclophilin A	gi 118102	1.36	0.11	7	6	A,B
	Cyclophilin B	gi 118090	1.42	0.07	6	5	A
Plasma membrane dynamic	Annexin I	gi 113944	1.25	0.04	8	8	A
	Annexin II	gi 113950	1.51	0.22	13	9	A,B
	Annexin A4	gi 1703319	1.58	0.15	8	7	A
	Annexin V	gi 113960	1.28	0.08	15	11	A
Stress response	Glucose-regulated protein 78 (GRP78)	gi 14916999	1.82	0.07	12	10	A
	Glucose-regulated protein 94 (GRP94)	gi 119360	1.51	0.08	13	11	A
	Oxygen-regulated protein (ORP150)	gi 10720185	1.55	0.12	12	12	A
	Protein disulfide isomerase (PDI) A3	gi 2507461	1.40	0.02	7	7	A
	Protein disulfide isomerase (PDI) A4	gi 119530	1.22	0.07	3	3	A
	Protein disulfide isomerase (PDI) A6	gi 2501205	1.24	0.10	4	4	A
	Calpain L1	gi 12408656	1.35	0.05	7	7	A
Antioxidant enzymes	Peroxiredoxin 2	gi 2507169	1.31	0.03	5	4	A
	Peroxiredoxin 5	gi 20141713	1.29	0.09	3	3	A
	Glutathione-*S*-transferase P (GST P)	gi 121746	1.31	0.10	5	5	A
	Glutathione-*S*-transferase omega 1	gi 4758484	2.79	0.21	4	3	A
Glycolysis, ATP generation and transport	Glyceraldehyde-3-phosphate dehydrogenase (GAPDH)	gi 120649	1.25	0.02	4	3	A,B
	Pyruvate kinase M1	gi 20178296	1.51	0.04	12	11	A,B
	Pyruvate kinase M2	gi 125604	1.48	0.05	8	7	A,B
	Lactate dehydrogenase A chain (LDH A)	gi 126047	1.33	0.12	10	7	A
	Lactate dehydrogenase B chain (LDH B)	gi 126041	1.36	0.06	4	3	A
	Isocitrate dehydrogenase (ICDH)	gi 20141568	1.30		2	1	A
	Mitochondrial ATP synthase α subunit	gi 114517	1.49	0.15	8	8	A
	Mitochondrial ATP synthase β subunit	gi 114549	1.42	0.08	18	14	A
	Adenine nucleotide translocator (ANT)	gi 113455	2.15	0.03	4	4	A
	Voltage-directed anion channel 1 (VDAC-1)	gi 130683	1.43	0.03	12	10	A
Others	Sialic acid synthase	gi 12056473	1.57	0.07	3	2	A
	Pyrroline-5-carboxylate synthase (P5CS)	gi 18574458	1.47	0.11	6	5	A
	Transgelin (SM 22a)	gi 586000	2.85	0.30	4	4	A
	ATP-dependent DNA helicase II, 70 kDa subunit (ku70)	gi 125729	1.26	0.04	10	10	A

[a] H:L ratio, intensity ratio of heavy isotope peak *versus* light isotope peak.
[b] S.D., standard deviation determined from quantification ratio from several peptides.
[c] A, μLC-nanospray-MS/MS; B, MALDI-TOF MS.

range of the detector. Whereas the S.D. of protein quantitations using isotope ratios could vary over a wide range (35), the S.D. of upregulated proteins listed in Table I were in the range of 0.02–0.27 based on multiple precursor-containing peptide signals for each protein quantitation. The average relative standard deviation (RSD) for the proteins listed in Table I was 6.1%. Thus, those proteins with changes in their expression levels of 20% or more were classified as the regulated proteins sensitive to p53 overexpression. Also, those proteins with expression level changes between 16 and 20% but with an RSD of less than 10% were considered as possible regulated proteins.

Furthermore, because of our use of multiple precursor-containing peptides for each protein quantitation, isozymes of the same enzyme family were unambiguously distinguished. For example, multiple peptides corresponding to either CypA or CypB were simultaneously identified and overlined in Fig. 1. The full-length sequence alignment showed that three human cyclophilin isozymes, CypA, CypB, and CypD, shared 31% sequence homology (Fig. 1). Four peptides identified for CypA (overlined in bold) showed consistent increases (1.36-fold) in the intensities of their heavy isotope peaks. None of the cysteine-containing peptides corresponding to CypA or CypB (Fig. 1) were observed directly in the MS analysis, suggesting

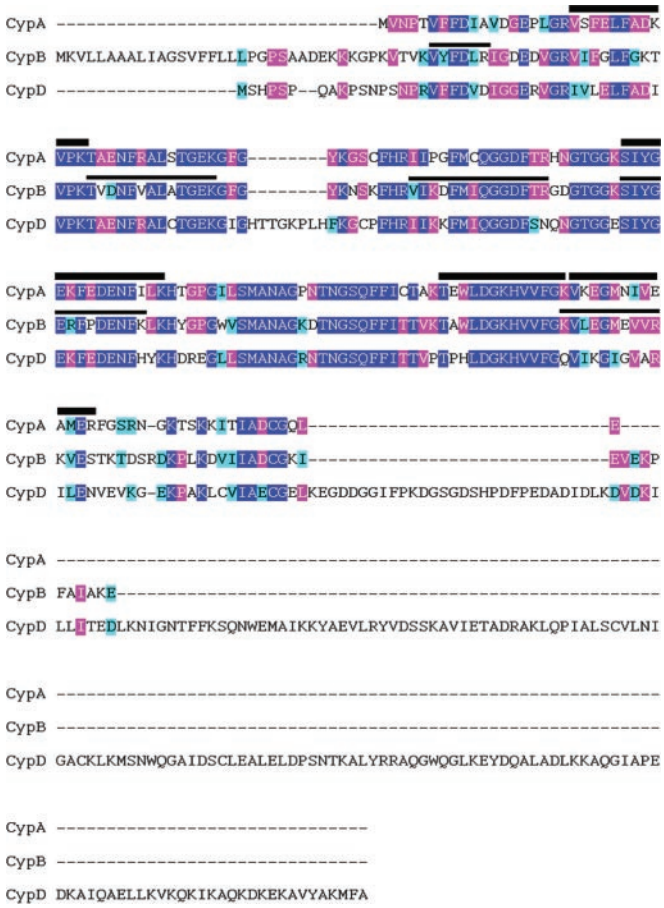

FIG. 1. **Sequence alignment of cyclophilin A, B, and D.** Protein sequences of CypA, B, and D were retrieved from GenBank™ under accession number P05092, P23284, and NP_005029, respectively. Conserved amino acid residues were highlighted using the Boxshade method (www.ch.embnet.org/software/BOX_doc.html). Identical residues in all three proteins are shaded in *blue*; identical residues in two of the three sequences are shaded in *magenta*; conserved residues were shaded in *green* background. Identified peptides that are matched to the sequence of CypA or CypB were overlined in the CypA or CypB sequence.

inefficient ionization or detection, possible posttranslational modifications of these peptides. This observation is reasonable because cysteine, on average, represents only 1.8% of cellular protein residues. It is noted that this AACT-based profile analysis requires only 100–300 μg of sample and is readily compatible with the online multiple-dimensional LC system for high-throughput analysis. Using multiple-dimensional separation coupled online with AACT will significantly reduce the sample preparation and analysis time and will make this approach more robust for large-scale and time-resolve analysis. Furthermore, software development for automatic validation of the identification and quantitation will greatly improve the throughput of data analysis.

Complimentary MALDI-based Profiling with Multiple AACT Precursors—Several low-abundance peptides were identified by the single-peptide-based AACT-MALDI approach but not by the LC-MS/MS approach. Although ESI-LC-MS/MS observes numerous peptide signals, some peptides were only detected by MALDI because of its different ionization mechanism. Furthermore, for those peptides that produce ambiguous MS/MS fragment signals or weak signals, MALDI peptide mass fingerprinting using multiple AACT precursors (30) is a powerful alternative and complementary approach. LC-MS/MS analysis may exclude extremely hydrophilic peptides that do not bind to the reverse-phase trapping column or certain extremely hydrophobic peptides that may not be eluted from the LC column under normal gradient condition.

Using various precursors such as leu-d_3, lys-d_4, met-d_3, and tyr-d_2 in parallel to mass-tag the proteome of DLD-1.p53 cells, 944 AACT peptides were detected by MALDI-TOF MS. Among them, 60 AACT peptides showed significant increases in the expression of their parent proteins in the apoptotic DLD-1.p53 cells. Their parent proteins were identified by their characteristic AACT mass-split patterns and amino acid compositions as described previously (30). The MALDI-TOF MS coupled with multiple AACT can greatly improve the specificity of peptide signals, thus enabling protein identification to be obtained from a single peptide. For example, in a digestion product from a gel band at 50 kDa, the peptide with an *m/z* 868.45 showed a 3-Da doublet isotope pattern for the met-d_3-labeled sample when compared with the unlabeled one, indicating one methionine in this peptide. Furthermore, the same peptide showed a 3-Da doublet isotope pattern in the leu-d_3-labeled sample, indicating one leucine in this peptide. The same peptide did not show specific isotope patterns for other labeled samples, indicating no lysine or tyrosine in this particular peptide. With this amino acid composition constraint, this peptide was assigned to the sequence MQHLIAR from pyruvate kinase (PK) M2 with a mass error of 80 ppm.

Among these proteins identified by AACT-MALDI TOF MS, the expression levels of several proteins were affected by p53 overexpression (Supplemental Table II). These up-regulated proteins such as cysteine dioxygenase, transcription repressor, and others are presumably of low abundance. These results showed how effectively this AACT-assisted MALDI-TOF MS method can complement MS/MS for generating more comprehensive quantitative protein profiles.

Using complementary AACT-LC-MS/MS and MALDI-TOF MS approaches, we found 81 proteins were up-regulated (Supplemental Table III) and 23 proteins were down-regulated (Supplemental Table IV) in response to p53 overexpression.

AACT-assisted De Novo Peptide Sequencing—The use of the leu-d_3 labels as an internal signature enhanced signal specificity for resolving residue ambiguities. For example, in MS/MS fragmentation of an up-regulated leu-d_3-containing peptide (Fig. 2*A*), the characteristic 3-Da mass-split pattern was continuously observed for its single- or double-charged daughter ions b8, b9 or y15 to y21 (Fig. 2*B*). The identical mass of 113.1 Da for both isoleucine and leucine makes it impossible to distinguish them in low-energy CID, whereas

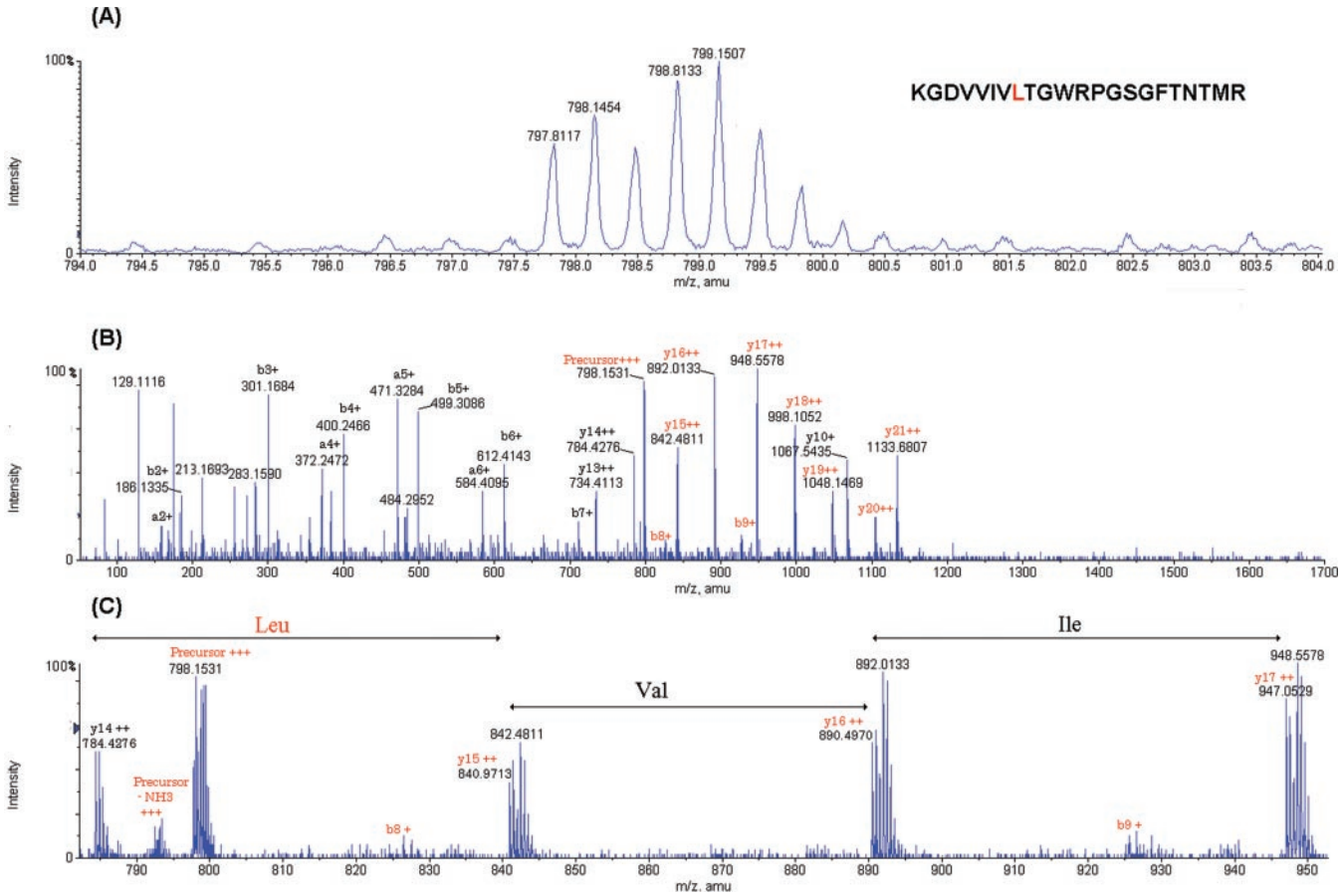

FIG. 2. **AACT quantitative analysis of a protein mixture.** A peptide signal from in-gel digestion mixture of a one-dimensional SDS-PAGE band. *A*, expanded view (*m/z* 794–804) of average TOF MS full scan (*m/z* 400–2,000) mass spectrum from time 24.65–24.95 min of the LC-MS analysis. *B*, MS/MS spectrum of the precursor ion in *panel A*. From a database search, this peptide was found to match to a tryptic peptide from PK. *C*, expanded view (*m/z* 780–955) of the spectrum in *panel B*.

the leucine-containing ions can be distinguished by the 3-Da mass-split of leu-d_3 tags. For example (Fig. 2*C*), the double-charged ions at *m/z* 947.05 and 890.49 were spaced by 113.1 Da, and both had a 3-Da mass-split pattern, showing that both ions contained a leucine. Therefore, the 113.1 Da mass loss for the 947.05 ion corresponds to the loss of an isoleucine residue. In contrast, the mass difference between the double-charged ions at *m/z* 840.97 and 784.42 was also 113.1 Da. However, the 3-Da mass-split pattern for the ion at 840.97 was not observed for the ion at 740.42, indicating clearly the loss of a leucine from 840.97. The peptide sequence of KGDVVIVLTGWRPGSGFTNTMR (PK) was therefore determined by using the leucine-constrained MASCOT or ProID database searching software.

In addition to lys-d_4-assisted *de novo* sequencing (29), the specific mass tags in MS/MS provided by other AACT labels were used to assign certain peptides/proteins from those poor-quality or incomplete fragment MS/MS spectra in this study. The signal specificity provided by "residue-specific tags" in large protein areas helps to resolve mass degeneracy and reduce spectral complexity in MS spectra of complex proteomes.

Use of Multiple AACT Precursors for Comprehensive Protein Quantitation—Some proteins were quantitated through the use of another precursor, lys-d_4, because of the absence of leucine in their MS-detectable peptides (Table II). A total of eight more proteins were quantitated, in which one was up-regulated, two were down-regulated, and the expression of another five proteins remained the same in the p53 overexpressed DLD-1 cells. It was also noted that in comparison with leu-d_3 labels, a lys-d_4 label has a 4-Da mass shift that overlaps less with the M+4 ion of the unlabeled peptide. Therefore, approximate protein expression levels could be quantified directly by the intensity difference between lys-d_4-labeled and unlabeled peptides. The combined sequence coverage of multiple leu-d_3- or lys-d_4-containing peptides has led to more precise protein quantitation and unambiguous identification of a larger number of the regulated proteins.

Functional Categorization of Some Up-regulated Proteins in Apoptotic DLD-1.p53 Cells—Table I shows that the up-regulated proteins fall into six major functional categories, including cell cycle arrest and p53 binding, protein chaperoning, plasma membrane dynamics, stress response, antioxidant

TABLE II
Additional proteins quantitated by lys-d_4-specific mass tagging

Accession no.	Protein description	Peptide	Quantification result
gi 133840	40S ribosmal protein S18	IAFAITAIK	Not changed
gi 20138086	Hypothetical Protein CGI-99	INEAIVAVQAIIADPK	Not changed
gi 18203506	Proteasome activator complex subunit	IEDGNDFGVAIQEK	Not changed
gi 5031931	Nascent-polypeptide-associated complex alpha polypeptide	SPASDTYIVFGEAK	Down-regulated 16%
gi 120749	Tumor-associated calcium signal transducer	TQNDVDIADVAYYFEK	Down-regulated 26%
gi 12804931	Acetyl-Coenzyme A acyltransferase 2	AANDAGYFNDEMAPIEVK	Up-regulated 39%
gi 631472	Translation initiation faactor eIF-4A2	GIYAYGFEKPSAIQQR	Not changed
gi 1136741	KIAA0002	AIADTGANVVVTGGK	Not changed

proteins, and glycolysis, ATP generation/transport. In addition to those previously identified by a variety of genomics approaches (12, 36), we found two cyclophilin isozymes, CypA and CypB, to be directly involved in p53-induced apoptosis. Furthermore, a number of proteins that are associated with hypoxia-induced apoptosis, such as annexins, oxygen regulated protein (ORP150), glucose regulated proteins (GRP78, GRP94), ATP-dependent DNA helicase II (or Ku70), glyceraldehyde-3-phosphate dehydrogenase (GAPDH), lactate dehydrogenase, and PK were also found to be up-regulated in the DLD-1.p53 cells. These observations support the view that hypoxia-induced apoptosis, in part, depends on the functions of p53 (37). The up-regulated proteins are found in different subcellular localizations. For example, annexins are known to be plasma membrane-associated, and both VDAC and ANT are mitochondrial-membrane associated. ORP150, GRP78, GRP94, and protein disulfide isomerases (PDIs) reside in the endoplasmic reticulum; cathepsin-L in the lysosome; and the glycolytic enzymes, HSP 27, 70, and 90 are cytosolic. As these proteins reside in different subcellular compartments and are differentially up-regulated by p53, it implies that p53-induced apoptosis is mediated through interorganelle crosstalk. The simultaneous identification of a number of antioxidant proteins (*e.g.* peroxiredoxin 2 and 5) up-regulated in the DLD-1.p53 cells suggested that p53 induces apoptosis, in part, through the generation of ROS and oxidative stress.

Some p53 Downstream Efectors Identified by AATC-MS Analysis Are Consistent with Previously Genomic Findings—As shown in Table I, the elevated expressions of 14-3-3-σ, Hsp27, and Hsp70 in the DLD-1.p53 cells were consistent with the results of previous genomic studies. 14-3-3-σ is known to be involved in cell cycle arrest and binding to p53 (38). Hsp27 and Hsp70 are known to be involved in p53-induced and stress-induced apoptosis (2, 39).

Proteins Previously Shown to Be Associated with p53-Induced Apoptosis Are Up-regulated—The expression levels of four annexins, namely I, II, A4 and V, were found to be elevated in the apoptotic DLD-1.p53 cells. Annexins belong to a family of structurally related proteins exhibiting Ca^{2+}-dependent binding activity to phospholipids. They are abundant, well-known biomarkers in apoptosis (40). Additionally, VDAC and ANT, the two major components of the permeability transition pore complex or the mitochondrial megachannel, were both up-regulated in apoptotic DLD-1.p53 cells. The

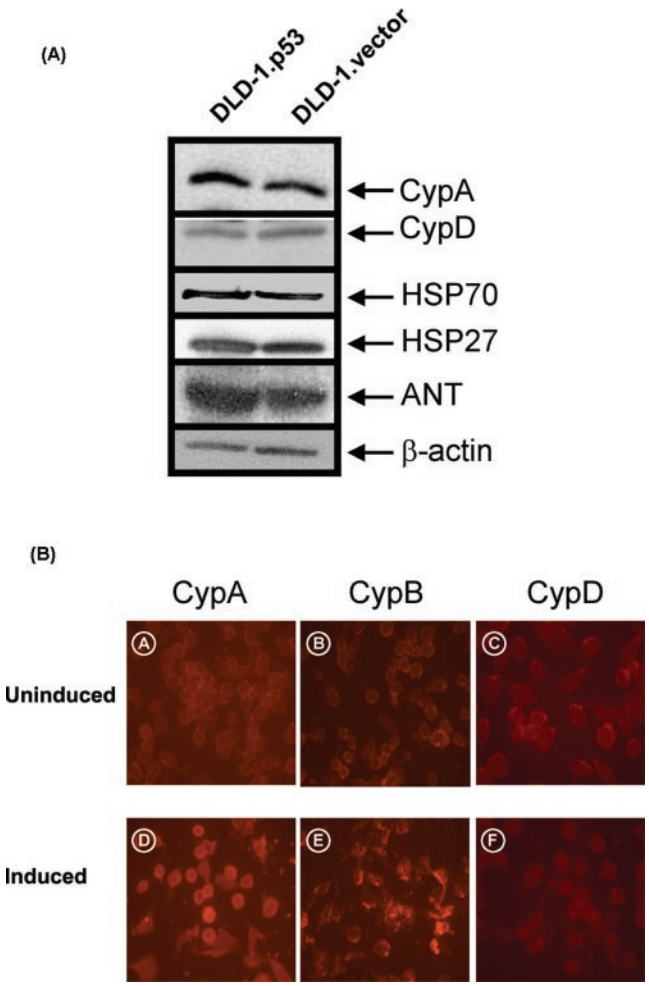

FIG. 3. **Immunoblotting analysis of some of the up-regulated proteins and immunofluorescent microscopy of cyclophilins.** *A*, total soluble proteins (30 μg each lane) were isolated from 22-h induced DLD-1.p53 or DLD-1.vector cells. Blots detected CypA and CypD, HSP70, HSP27, and ANT. β-actin was used for the loading control. *B*, fluorescent photomicrographs of normal and apoptotic DLD-1.p53 cells immunostained with antibody against CypA (*A* and *D*), CypB (*B* and *E*), and CypD (*C* and *F*).

permeability transition pore complex is formed at the interface site between the outer mitochondrial membrane and the inner mitochondrial membrane, and contains several classes of transmembrane proteins, *i.e.* the VDAC, the ANT, and the peripheral benzodiazepine receptor (PBR). It is also associated with members of the Bcl-2 family (*e.g.* BAX), as well as hexokinase II, mitochondrial creatine kinase, and CypD (6, 41, 42). Direct interactions have been shown between ANT and CypD, as well as between the ANT and VDAC (6, 43). Lin and Lechleiter (44) have shown that overexpression of CypD desensitizes HEK293 cells to apoptotic stimuli, implying that CypD possesses a cell survival/protective role against apoptosis. Finally, a recent study by Schubert (45) showed that CypD is an apoptosis repressor.

Functional Validation of Newly Identified Proteins That Are Up-regulated in the Apoptotic DLD-1.p53 Cells—Immunoblotting and immunofluorescent microscopy experiments were conducted to determine the expression changes of CypA, CypB, and CypD in apoptotic DLD-1.p53 cells. As shown in Fig. 3*A*, the immunoblots indicated that the expression level of CypA, but not CypD, was increased in apoptotic DLD-1.p53 cells compared with the normal DLD-1 cells. In addition, the immunofluorescent assay also showed that the intracellular levels of both CypA and CypB, but not CypD, increased in apoptotic DLD-1.p53 cells (Fig. 3*B*). As indicated above, CypD possesses cell survival activity. Therefore, that its expression level remained unchanged in apoptotic DLD-1.p53 cells is reasonable. CypA, also known as peptidyl-prolyl cis/trans isomerase A (PPIase A), was originally identified as a major intracellular receptor for the immunosuppressant cyclosporin A (46). The PPIase family of proteins catalyzes the cis/trans isomerization of the peptide bond N-terminal to proline and is believed to regulate the activities of mature proteins by promoting assembly or intercellular transportation of their subunits via such isomerizations (47). Recent studies showed that Pin1, one of the PPIase family members, can bind and change the conformation of phosphorylated p53, displacing HDM2, a p53 binding protein, thus stabilizing and activating p53 (48, 49). It is theoretically possible that other PPIases, such as CypA and CypB, may function similarly on p53. Finally, it has been shown that CypA is involved in excitotoxin-induced caspase activation and apoptosis in rat neuronal B50 cells (50, 51). In immunoblotting experiments, we also showed that ANT, Hsp27, and Hsp70 were up-regulated in the apoptotic DLD-1.p53 cells, in agreement with the results of AACT-MS analysis (Fig. 3*A*).

It is noteworthy that mitochondria have been shown to be the "executioner" in p53-induced apoptosis. Mitochondrial regulation of apoptosis has been described at several levels: 1) maintenance of ATP production; 2) maintenance of NAD(P)+/NAD(P)H homeostasis; and 3) alteration of MMP and permeability pore (PT) for the release of apoptogenic factors (6, 41–43, 52). PT, also known as the "megachannel,"

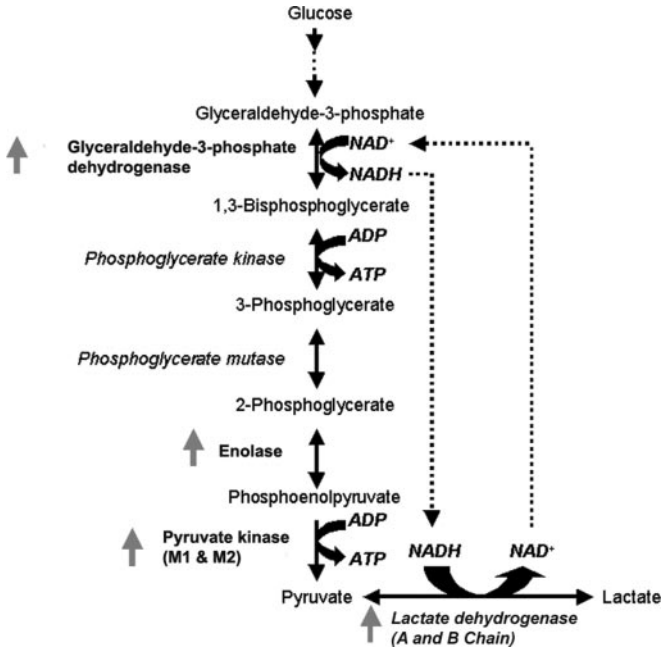

FIG. 4. **Up-regulated enzymes in anaerobic glycolysis in p53-induced apoptosis.** Glyceraldehyde-3-phosphate dehydrogenase, enolase, PK (both M1 and M2 isoforms), and lactate dehydrogenase (both A and B chains) were simultaneously up-regulated in apoptotic DLD-1.p53 cells.

is thought to consist of the VDAC, ANT, and CypD. Its opening is regulated by both MMP and by the pH of the mitochondrial matrix and is the site of the release of apoptogenic factors (41, 42, 52). Identification of the up-regulation of CypA, CypB, VDAC, and ANT, but not of CypD, in p53-induced apoptosis in DLD-1 cells implies that these proteins are involved in the alteration of MMP and the function of PT opening in mitochondria-mediated apoptosis.

Identification of Stress-response Proteins in Response to ROS Generation—When sensing oxidative stress, cells respond with an increase of antioxidation activity in order to neutralize ROS. In our quantitative proteomic dataset, at least 15 of the up-regulated proteins are associated with the oxidative stress response and antioxidant activities. For example, peroxiredoxin 2 and 5, also known as glutathione peroxidases, are bifunctional enzymes possessing both glutathione peroxidase and phospholipase A2 activities (53–55). These enzymes catalyze the conversion of peroxides to H_2O and O_2 and are induced by oxidative stress (55). It has been reported that a major cellular response to oxidative stress is the oxidative modification of peroxiredoxins. Peroxiredoxins control cellular redox status by reacting with ROS using their intramolecular cysteine residue(s) that both buffers and eliminates ROS toxicity. These oxidizing reactions are reversible when intracellular redox is balanced (53–55). Using proteomic analysis, Rabilloud and colleagues (56) showed that peroxiredoxins are subjected to *in vitro* overoxidation at their active site in response to oxidative stress. Additionally, two well-known

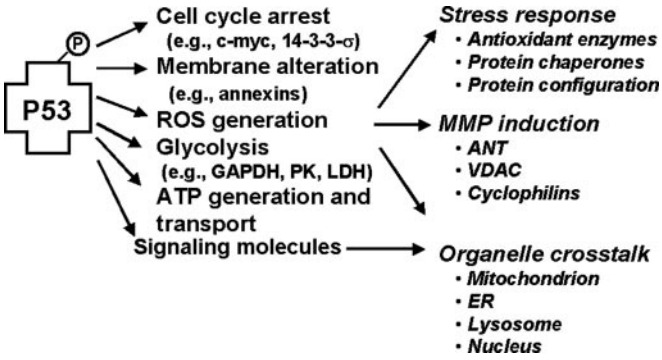

FIG. 5. **Global view of multipathway p53-induced apoptosis in DLD-1 cells on the basis of this quantitative proteomic dataset.**

antioxidation enzymes, glutathione *S*-transferases (GST) P and omega 1, were also identified by our proteomic analysis (Table I). Our finding of at least 15 antioxidant proteins underscores the notion that p53-induced apoptosis is, in part, mediated through the generation of ROS and oxidative stress (3, 9). It is noteworthy that several stress-response and cell protector proteins can turn into pro-apoptotic killers in some cell types under different physiologic conditions. For example, overexpression of Hsp70 is apoptogenic (39), and anti-apoptotic protein Bcl-2 can be converted to pro-apoptotic killer by interacting with the nuclear receptor TR3 (57). However, the molecular mechanisms underlying these interesting phenomena are not understood. In addition, as our original goal was to identify regulated protein in the execution (late) stage of p53-induced apoptosis, we figured that some of the regulated proteins might not be the direct targets of p53 but rather the secondary effectors responsive to p53-initiated signaling network in apoptosis.

Four Enzymes Involved in Anaerobic Glycolysis Are Up-regulated in the Apoptotic DLD-1.p53 Cells—We found that four glycolytic enzymes, GAPDH, PK, lactate dehydrogenase, and α-enolase, were up-regulated by 19–50% during p53-induced apoptosis (Fig. 4, Table I, Supplemental Table III). Recently, glycolytic enzymes, such as GAPDH and glucokinase (GK), have been shown to be regulators in gene expression and apoptosis. For example, Zheng and colleagues (58) showed that a nuclear form of GAPDH is a key component of the nuclear OCA-S complex that is essential for S phase-dependent histone H2B gene transcription. Daniel and colleagues (59) showed that the pro-apoptotic protein BAD formed a mitochondrially located complex with GK as well as protein kinase A (PKA), protein phosphatase 1 and a PKA-anchoring protein, WAVE-1. These proteins are known to influence apoptosis (*e.g.* BAX, PKA) and glucose metabolism (*e.g.* GK). GK, highly expressed in the liver and pancreas, catalyzes the phosphorylation of glucose to glucose 6-phosphate—the first and the rate-limiting step in several pathways of glucose metabolism, including glycolysis and glycogen synthesis. We did not detect GK peptides, possibly due to the low-abundance of GK in the DLD-1 cells derived from a colorectal tumor. However, PK, the other rate-limiting enzyme that regulates the progress of glycolysis, was identified by our proteomic assay. Both M1 and M2 isozymes of PK were up-regulated about 50% in the DLD-1.p53 cells. Therefore, systematic identification of these four glycolytic enzymes, especially PK, revealed additional links between glucose metabolism and apoptosis. It is also well documented that apoptotic pathways are highly energy demanding and ATP-dependent (42). Our finding of the up-regulation of PK supports this notion and further suggests that the induction of ATP-generating enzymes is specific. Several ATP-generating systems enzymes (α and β subunits of ATP synthase of mitochondrial F1 complex, isocitrate dehydrogenase, malate dehydrogenase, and cysteine dioxygenase) were also up-regulated (Table I, Supplemental Table III). Finally, the PK M2 isoform has been a diagnosis biomarker in several cancers (60). Identification of another PK isoform, M1, that was up-regulated by p53 in apoptosis, is novel.

As summarized in Fig. 5, this systemic study of the proteomes of apoptotic *versus* normal cells has identified multiple players that are involved in multiple pathways at the execution stage of p53-induced apoptosis. For the first time, our findings of large-scale profiling provide new insights into a global view of p53-induced apoptosis.

Acknowledgments—We thank Bert Vogelstein for kindly providing us with he cell lines, DLD-1.p53, and DLD-1.vector and Robert Glew for critical reading of this manuscript.

* This work is supported by Los Alamos National Laboratory Directed Research Development (LDRD) 20030508ER, DOE Grants ERW9840, ERW9923 (to X. C.), Howard Hughes Medical Institute Research grant-in-aid to the University of New Mexico Cancer Research Facility, and American Cancer Society Institutional Research Grant (ACS-IRG #412488-00095) (to C.-A. A. H.). X. C. is a recipient of Presidential Early Career Award for Scientists and Engineers (2000–2005). The costs of publication of this article were defrayed in part by the payment of page charges. This article must therefore be hereby marked "*advertisement*" in accordance with 18 U.S.C. Section 1734 solely to indicate this fact.

S The on-line version of this manuscript (available at http://www.mcponline.org) contains supplemental material.

§ S. G. and Z. L. contributed equally to this work.

‡‡ To whom correspondence should be addressed: Xian Chen, MS M888, B-2, Bioscience Division, Los Alamos National Laboratory, Los Alamos, NM 87545. E-mail: chen_xian@lanl.gov. Chien-An A. Hu, Department of Biochemistry and Molecular Biology, University of New Mexico Health Science Center, Albuquerque, NM 87131. E-mail: ahu@salud.unm.edu.

REFERENCES

1. Hengartner, M. O. (2000) The biochemistry of apoptosis. *Nature* **407,** 770–776
2. Ferri, K. F., and Kroemer, G. (2001) Organelle-specific initiation of cell death pathways. *Nat. Cell Biol.* **3,** E255–E263
3. Johnson, T. M., Yu, Z. X., Ferrans, V. J., Lowenstein, R. A, and Finkel, T. (1996) Reactive oxygen species are downstream mediators of p53-dependent apoptosis. *Proc. Natl. Acad. Sci. U. S. A.* **93,** 11848–11852
4. Vila, M., and Przedborski, S. (2003) Targeting programmed cell death in neurodegenerative diseases. *Nat. Rev. Neurosci.* **4,** 365–375

5. Scorrano, L., and Korsmeyer, S. J. (2003) Mechanisms of cytochrome c release by proapoptotic BCL-2 family members. *Biochem. Biophys. Res. Commun.* **304,** 437–444
6. Newmeyer, D. D., and Ferguson-Miller, S. (2003) Mitochondria: Releasing power for life and unleashing the machineries of death. *Cell* **112,** 481–490
7. Vogelstein, B., Lane, D., and Levine, A. J. (2000) Surfing the p53 network. *Nature* **408,** 307–310
8. Vousden, K. H., and Lu, X. (2002) Live or let die: the cell's response to p53. *Nat. Rev. Cancer* **2,** 594–604
9. Polyak, K., Xia, Y., Zweier, J. L., Kinzler, K. W., and Vogelstein, B. (1997) A model for p53-induced apoptosis. *Nature* **389,** 300–305
10. Donald, S. P., Sun, X. Y., Hu, C. A., Yu, J., Mei, J. M., Valle, D., and Phang, J. M. (2001) Proline oxidase, encoded by p53-induced gene-6, catalyzes the generation of proline-dependent reactive oxygen species. *Cancer Res.* **61,** 1810–1815
11. Maxwell, S. A., and Rivera, A. (2003) Proline oxidase induces apoptosis in tumor cells, and its expression is frequently absent or reduced in renal carcinomas. *J. Biol. Chem.* **278,** 9784–9789
12. Yu, J., Zhang, L., Hwang, P. M., Rago, C., Kinzler, K. W., and Vogelstein, B. (1999) Identification and classification of p53-regulated genes. *Proc. Natl. Acad. Sci. U. S. A.* **96,** 14517–14522
13. Amundson, S. A., Bittner, M., Meltzer, P., Trent, J., and Fornace, A. J., Jr. (2001) Physiological function as regulation of large transcriptional programs: The cellular response to genotoxic stress. *Comp. Biochem. Physiol B Biochem. Mol. Biol.* **129,** 703–710
14. Israeli, D., Tessler, E., Haupt, Y., Elkeles, A., Wilder, S., Amson, R., Telerman, A., and Oren, M. (1997) A novel p53-inducible gene, PAG608, encodes a nuclear zinc finger protein whose overexpression promotes apoptosis. *EMBO J.* **16,** 4384–4392
15. el-Deiry, W. S., Tokino, T., Velculescu, V. E., Levy, D. B., Parsons, R., Trent, J. M., Lin, D., Mercer, W. E., Kinzler, K. W., and Vogelstein, B. (1993) WAF1, a potential mediator of p53 tumor suppression. *Cell* **75,** 817–825
16. Chen, G., Gharib, T. G., Huang, C. C., Taylor, J. M., Misek, D. E., Kardia, S. L., Giordano, T. J., Iannettoni, M. D., Orringer, M. B., Hanash, S. M., and Beer, D. G. (2002) Discordant protein and mRNA expression in lung adenocarcinomas. *Mol. Cell. Proteomics* **1,** 304–313
17. Washburn, M. P., Koller, A., Oshiro, G., Ulaszek, R. R., Plouffe, D., Deciu, C., Winzeler, E., and Yates, J. R., III. (2003) Protein pathway and complex clustering of correlated mRNA and protein expression analyses in *Saccharomyces cerevisiae*. *Proc. Natl. Acad. Sci. U. S. A.* **100,** 3107–3112
18. Gygi, S. P., Rochon, Y., Franza, B. R., and Aebersold, R. (1999) Correlation between protein and mRNA abundance in yeast. *Mol. Cell. Biol.* **19,** 1720–1730
19. Aebersold, R., and Mann, M. (2003) Mass spectrometry-based proteomics. *Nature* **422,** 198–207
20. Pandey, A., and Mann, M. (2000) Proteomics to study genes and genomes. *Nature* **405,** 837–846
21. Gygi, S. P., Rist, B., Gerber, S. A., Turecek, F., Gelb, M. H., and Aebersold, R. (1999) Quantitative analysis of complex protein mixtures using isotope-coded affinity tags. *Nat. Biotechnol.* **17,** 994–999
22. Tao, W. A., and Aebersold, R. (2003) Advances in quantitative proteomics via stable isotope tagging and mass spectrometry. *Curr. Opin. Biotechnol.* **14,** 110–118
23. Chen, X., Smith, L. M., and Bradbury, E. M. (2000) Site-specific mass tagging with stable isotopes in proteins for accurate and efficient protein identification. *Anal. Chem.* **72,** 1134–1143
24. Ong, S. E., Blagoev, B., Kratchmarova, I., Kristensen, D. B., Steen, H., Pandey, A., and Mann, M. (2002) Stable isotope labeling by amino acids in cell culture, SILAC, as a simple and accurate approach to expression proteomics. *Mol. Cell. Proteomics* **1,** 376–386
25. Gu, S., Pan, S., Bradbury, E. M., and Chen, X. (2003) Precise peptide sequencing and protein quantification in the human proteome through *in vivo* lysine-specific mass tagging. *J. Am. Soc. Mass Spectrom.* **14,** 1–7
26. Zhu, H., Pan, S., Gu, S., Bradbury, E. M., and Chen, X. (2002) Amino acid residue specific stable isotope labeling for quantitative proteomics. *Rapid Commun. Mass Spectrom.* **16,** 2115–2123
27. Ong, S. E., Foster, L. J., and Mann, M. (2003) Mass spectrometric-based approaches in quantitative proteomics. *Methods* **29,** 124–130
28. Yu, J., Zhang, L., Hwang, P. M., Kinzler, K. W., and Vogelstein, B. (2001) PUMA induces the rapid apoptosis of colorectal cancer cells. *Mol. Cell* **7,** 673–682
29. Gu, S., Pan, S., Bradbury, E. M., and Chen, X. (2002) Use of deuterium-labeled lysine for efficient protein identification and peptide *de novo* sequencing. *Anal. Chem.* **74,** 5774–5785
30. Pan, S., Gu, S., Bradbury, E. M., and Chen, X. (2003) Single peptide-based protein identification in human proteome through MALDI-TOF MS coupled with amino acids coded mass tagging. *Anal. Chem.* **75,** 1316–1324
31. Gu, S., Chen, J., Dobos, K M., Bradbury, E. M., Belisle, J. T., and Chen, X. (2003) Comprehensive proteomic profiling of the membrane constituents of a *Mycobacterium tuberculosis* strain. *Mol. Cell. Proteomics* **2,** 1284–1296
32. Perkins, D. N., Pappin, D. J., Creasy, D. M., and Cottrell, J. S. (1999) Probability-based protein identification by searching sequence databases using mass spectrometry data. *Electrophoresis* **20,** 3551–3567
33. Peng, J., Elias, J. E., Thoreen, C. C., Licklider, L. J., and Gygi, S. P. (2003) Evaluation of multidimensional chromatography coupled with tandem mass spectrometry (LC/LC-MS/MS) for large-scale protein analysis: The yeast proteome. *J. Proteome Res.* **2,** 43–50
34. Shevchenko, A., Sunyaev, S., Loboda, A., Shevchenko, A., Bork, P., Ens, W., and Standing, K. G. (2001) Charting the proteomes of organisms with unsequenced genomes by MALDI-quadrupole time-of-flight mass spectrometry and BLAST homology searching. *Anal. Chem.* **73,** 1917–1926
35. Blagoev, B., Kratchmarova, I., Ong, S. E., Nielsen, M., Foster, L. J., and Mann, M. (2003) A proteomics strategy to elucidate functional protein-protein interactions applied to EGF signaling. *Nat. Biotechnol.* **21,** 315–318
36. Xu, H., and el-Gewely, M. R. (2001) P53-responsive genes and the potential for cancer diagnostics and therapeutics development. *Biotechnol. Annu. Rev.* **7,** 131–164
37. Harris, A. L. (2002) Hypoxia—A key regulatory factor in tumour growth. *Nat. Rev. Cancer* **2,** 38–47
38. Hermeking, H., Lengauer, C., Polyak, K., He, T. C., Zhang, L., Thiagalingam, S., Kinzler, K. W., and Vogelstein, B. (1997) 14-3-3 sigma is a p53-regulated inhibitor of G_2/M progression. *Mol. Cell* **1,** 3–11
39. Takayama, S., Reed, J. C., and Homma, S. (2003) Heat-shock proteins as regulators of apoptosis. *Oncogene* **22,** 9041–9047
40. Reutelingsperger, C. P., Dumont, Em, Thimister, P. W., van Genderen, H., Kenis, H., van de Eijnde, S., Heidendal, G., and Hofstra, L. (2002) Visualization of cell death *in vivo* with the annexin A5 imaging protocol. *J. Immunol. Methods* **265,** 123–132
41. Zamzami, N., and Kroemer, G. (2001) The mitochondrion in apoptosis: How Pandora's box opens. *Nat. Rev. Mol. Cell Biol.* **2,** 67–71
42. Mayer, B., and Oberbauer, R. (2003) Mitochondrial regulation of apoptosis. *News Physiol. Sci.* **18,** 89–94
43. Belzacq, A. S., Vieira, H. L., Kroemer, G., Brenner, C. (2002) The adenine nucleotide translocator in apoptosis. *Biochimie* **84,** 167–176
44. Lin, D. T., and Lechleiter, J. D. (2002) Mitochondrial targeted cyclophilin D protects cells from cell death by peptidyl prolyl isomerization. *J. Biol. Chem.* **277,** 31134–31141
45. Schubert, A., and Grimm, S. (2004) Cyclophilin D, a component of the permeability transition-pore, is an apoptosis repressor. *Cancer Res.* **64,** 85–93
46. Bukrinsky, M. I. (2002) Cyclophilins: Unexpected messengers in intercellular communications. *Trends Immunol.* **23,** 323–325
47. Ansari, H., Greco, G., and Luban, J. (2002) Cyclophilin A peptidyl-prolyl isomerase activity promotes ZPR1 nuclear export. *Mol. Cell. Biol.* **22,** 6993–7003
48. Zheng, H., You, H., Zhou, X. Z., Murray, S. A., Uchida, T., Wulf, G., Gu, L., Tang, X., Lu, K. P., and Xiao, Z. X. (2002) The prolyl isomerase Pin1 is a regulator of p53 in genotoxic response. *Nature* **419,** 849–853
49. Zacchi, P., Gostissa, M., Uchida, T., Salvagno, C., Avolio, F., Volinia, S., Ronai, Z., Blandino, G., Schneider, C., and Del Sal, G. (2002) The prolyl isomerase Pin1 reveals a mechanism to control p53 functions after genotoxic insults. *Nature* **419,** 853–857
50. Jin, Z. G., Gostissa, M., Uchida, T., Salvagno, C., Avolio, F., Volinia, S., Ronai, Z., Blandino, G., Schneider, C., and Del Sal, G. (2000) Cyclophilin A is a secreted growth factor induced by oxidative stress. *Circ. Res.* **87,** 789–796
51. Capano, M., Virji, S., and Crompton, M. (2002) Cyclophilin-A is involved in excitotoxin-induced caspase activation in rat neuronal B50 cells. *Biochem. J.* **363,** 29–36

52. Henry-Mowatt, J., Dive, C., Martinou, J. C., and James, D. (2004) Role of mitochondrial membrane permeabilization in apoptosis and cancer. *Oncogene* **23,** 2850–2860
53. Chen, J. W., Dodia, C., Feinstein, S. I., Jain, M. K., and Fisher, A. B. (2000) 1-Cys peroxiredoxin, a bifunctional enzyme with glutathione peroxidase and phospholipase A2 activities. *J. Biol. Chem.* **275,** 28421–28427
54. Butterfield, L. H., Merino, A., Golub, S. H., and Shau, H. (1999) From cytoprotection to tumor suppression: The multifactorial role of peroxiredoxins. *Antioxid. Redox Signal* **1,** 385–402
55. Wood, Z. A., Schroder, E., Robin Harris, J., and Poole, L. B. (2003) Structure, mechanism and regulation of peroxiredoxins. *Trends Biochem. Sci*. **28,** 32–40
56. Rabilloud, T., Heller, M., Gasnier, F., Luche, S., Rey, C., Aebersold, R., Benahmed, M., Louisot, P., and Lunardi, J. (2002) Proteomics analysis of cellular response to oxidative stress. Evidence for in vivo overoxidation of peroxiredoxins at their active site. *J. Biol. Chem.* **277,** 19396–19401
57. Lin, B. Z., Kolluri, S. K., Lin, F., Liu, W., Han, Y. H., Cao, X., Dawson, M. I., Reed, J. C., and Zhang, X. K. (2004) Conversion of Bcl-2 from protector to killer by interaction with nuclear orphan receptor Nur77/TR3. *Cell* **116,** 527–540
58. Zheng, L., Roeder, R. G., and Luo, Y. (2003) S phase activation of the histone H2B promoter by OCA-S, a coactivator complex that contains GAPDH as a key component. *Cell* **114,** 255–266
59. Danial, N. N., Gramm, C. F., Scorrano, L., Zhang, C. Y., Krauss, S., Ranger, A. M., Datta, S. R., Greenberg, M. E., Licklider, L. J., Lowell, B. B., Gygi, S. P., and Korsmeyer, S. J. (2003) BAD and glucokinase reside in a mitochondrial complex that integrates glycolysis and apoptosis. *Nature* **424,** 952–956
60. Hoopmann, M., Warm, M., Mallmann, P., Thomas, A., Gohring, U. J., and Schondorf, T. (2002) Tumor M2 pyruvate kinase—Determination in breast cancer patients receiving trastuzumab therapy. *Cancer Lett.* **187,** 223–228